Heterogeneity of Spine Density in Pyramidal Neurons of Isocortex of Mongoose, *Herpestes edwardsii* (É. Geoffroy Saint-Hilaire 1818)

U.C. SRIVASTAVA,* SIPPY SINGH, AND PRASHANT CHAUHAN
Department of Zoology, University of Allahabad, Allahabad 211002, India

KEY WORDS interlaminar; interregional; frontal; temporal; parietal; occipital

ABSTRACT The characteristics of pyramidal neurons within six layers of Indian gray mongoose (*Herpestes edwardsii*) isocortex have been investigated using Golgi and Cresyl-Violet methods. Pyramidal neurons and the cytoarchitecture of isocortex of mongoose were photographed with the help of computer aided Nikon eclipse 80i microscope whereas the lucida drawings were made by simple light microscope equipped with camera lucida. The cortical neurons exhibit marked regional differences in phenotype. The differences occur in morphology and distribution of spines within the cortical neurons not only among different species but also within an animal's brain. The present investigation aims at studying the features of pyramidal neurons and to find out the differences if any in distribution of spines in different layers (II–VI) as well as regions (Frontal, Temporal, Parietal, and Occipital) of isocortex of mongoose, which will provide information regarding importance of different layer and region. This piece of work embarks the findings that spine density shows inter-regional as well as interlaminar variations within isocortex of mongoose indicating that pyramidal cells present in varied layer and region are not equally functional and there do exists differences in activity among layers and regions. Among regions, the Temporal region possessing highest spine density contributes more toward functioning of mongoose isocortex and might play significant role in predatory nature of mongoose because this region in mammals is associated with auditory, visual perception, and object recognition. *Microsc. Res. Tech. 76:818–828, 2013*.

INTRODUCTION

The cytoarchitecture of the cerebral cortex in mammals has been conventionally investigated using Nissl, Golgi, or myelin stains. Most available studies on neuronal subtypes identified by their molecular and morphologic characteristics have been performed in species commonly used in laboratory research such as the rat, mouse, cat, and monkey, as well as in autopsic human brain specimens. Many studies have been done hitherto on neuronal types present in mammalian isocortices representing various orders by using Golgi method and Nissl staining methods viz. on human (Von Economo, 1927); dog (Tunturi, 1971); cat (Gilbert and Kelly, 1975; Mitra, 1955); monkey (Garey and Saini, 1981; Lund et al., 1979); and dolphin (Garey et al., 1985). Ferrer et al. (1986) performed a wide study on neuronal structural form and cellular distribution in the Layer VI of the cerebral cortex by Golgi method on gyrencephalic and lissencephalic brains of mammals representing various orders viz. carnivora, artiodactyla, primate, rodentia, lagomorpha, insectivora, and chiroptera. Later Ferrer et al. (1987) revealed the changing capabilities related to cortical folding of neurons of Layer VI under normal and abnormal developmental conditions in different mammalian orders. Other prominent Golgi and Nissl studies described morphological features of Layer V pyramidal neurons in rat neocortex (Chagnac-Amitai et al., 1990); the cell type in auditory cortex of mustached bat (Fitzpatrick and Henson, 1994); pyramidal cell dendritogenesis in ferret (Zervas and Walkley, 1999); heterogeneity in dendritic tree pattern of pyramidal neurons in visual areas of marmoset monkeys (Elston et al., 1999); neuroarchitechture of auditory cortex in horseshoe bat (Radtke-Schuller, 2001); morphology of pyramidal cells in different cortex of owl monkey (Elston, 2003) and visual cortex of tree shrew (Elston et al., 2005); neuronal classes in the isocortex of echidna (Hassiotis and Ashwell, 2003); and morphological differences in pyramidal neurons in parietal lobe of mongoose (Srivastava and Chauhan, 2010).

Cortical neurons exhibit a differential distribution among cortical layers and regions, and some of them are differentially represented among species (Hof et al., 1999). In mustached bat auditory cortex, the laminar proportions and distribution of cell types were different from those reported in primary sensory cortex of other species (Fitzpatrick and Henson, 1994).

*Correspondence to: U.C. Srivastava, Department of Zoology, University of Allahabad, Allahabad 211002, India. E-mail: ucsrivastava@redffmail.com

Received 25 February 2013; accepted in revised form 5 May 2013

Contract grant sponsor: Council of Scientific and Industrial Research (CSIR) fellowship; Contract grant number: F. No.10-2(5)/2006(i)-E.U. II; Contract grant sponsor: University Grants Commission (UGC) Fellowship; Contract grant number: 20-6/2008(ii)EU-IV.

DOI 10.1002/jemt.22234
Published online 3 June 2013 in Wiley Online Library (wileyonlinelibrary.com).

Similarly, dendritic architecture of Layers II/III pyramidal neurons located in secondary somatosensory, lateral secondary motor, lateral secondary visual, and association temporal cortex was found to differ characteristically in rat which shows that each cortical region is built with specific neuronal components (Benavides-Piccione et al., 2006).

Typical mammalian pyramidal neurons possess dendritic spines, a characteristic feature which represents important structural specializations of isocortical neurons of eutherians providing maximum post-synaptic sites of axon terminating upon pyramidal neurons (Feldman, 1984; Nieuwenhuys, 1994). Differences in spine density of pyramidal neurons might reflect functional differences within the isocortex. Differences in density of dendritic spines and length of spines were found to be significant between somatosensory and motor cortex of echidna and rat (Hassiotis and Ashwell, 2003) and in spine density of pyramidal neurons of visual areas in marmoset monkey (Elston et al., 1999). Interlaminar variations in spine density of pyramidal neurons have been reported in bat (Srivastava and Pathak, 2010) and squirrel (Srivastava and Srivastava, 2011) but the results were confined to Parietal region only.

Mongoose, chosen for this study belongs to superfamily Feloidea which represents the most modified carnivores. It shows many of the characters possessed by feloids in the Oligocene. In general, they are like the ancestral miacids, with long skull, small brain, and short legs. Despite this, previous studies have confined to general carnivore animal models like cat, dog, and ferret (without considering the distribution of spines in pyramidal neurons among all the regions and layers of isocortex) with no study ever been performed on neuronal classes of mongoose. Hence this fairly intelligent and inquisitive carnivore—mongoose was selected as animal model for the present study. The main objective of the present investigation is to study the features of pyramidal neurons and to find out the differences if any in distribution of spines in different layers as well as regions of isocortex of mongoose, which will provide information regarding the importance of different layers and regions. The observations from mongoose isocortex have been compared with those from prototherian and other eutherian mammals reported earlier.

MATERIALS AND METHODS

A total of three adult male mongooses, *Herpestes edwardsii* (sanctioned by ethical committee) were used in the present study. Animals were captured from the surroundings of Allahabad (25° 28′ N, 81° 54′ E) (Uttar Pradesh, India), and kept in terrarium prior to the experiments. The common Indian gray mongoose could be observed in areas of thickets, in cultivated fields or in broken, bushy vegetation, open areas, grasslands, and scrubs. They have long bodies, short legs, and highly developed anal scent glands. *H. edwardsii* could be identified by its silver-gray, salt-and-pepper speckled fur, and white-tipped tail. The animals selected for the study were 38–46 cm long, with about 35 cm long tail. The weight ranged from 3–4 kg. All the experiments were carried in concordance with the animal care guidelines of the Animal Ethical Committee of Department of Zoology, University of Allahabad, Allahabad.

Three anaesthetized adult mongooses were perfused transcardially with 500 mL of physiological saline followed by a fixative solution consisting of 4% paraformaldehyde in 0.1 M phosphate buffer (4°C, pH 7.4) for 1 h. Brain was immediately taken out from the skull and post fixed in the fixative solution for 24 h at 4°C. The methods employed are:

1. Cresyl Violet method
   Small blocks 5 mm thick were removed from both hemispheres of the brain for Cresyl Violet staining. The pieces of brain were thoroughly washed with distilled water to remove the excess fixative agent, then dehydrated through ascending grades of alcohol, i.e. 50%, 70%, 90%, and 100% alcohols for 15 min in each grade followed by a 15 min immersion in a 1:1 mixture of absolute alcohol and xylene. They were cleared in xylene for 5–10 min and then transferred to a mixture of xylene and molten paraffin wax (m.p. 56–58°C) at 56°C for 30 min. After this, the pieces were transferred to pure molten paraffin wax (m.p. 56–58°C) at 56°C for 4 h (3 changes of 1, 1, and 2 h each). Finally, they were embedded in pure molten paraffin wax (m.p. 56–58°C). The blocks were sectioned at a thickness of 10 μm on a rotatory microtome and further deparaffinized in xylene for 20 min (two changes, 10 min each). The sections were treated with descending grades of alcohol, i.e. 100%, 90%, 70%, and 50% alcohol (10 min each) and then washed in distilled water. The sections were then stained with 0.1% Cresyl violet (2–5 minutes) for purpose of identifying cortical layers and cytoarchitectural features of isocortical region. After this, the sections were washed in distill water and then rinsed with ascending grades of alcohol (50%, 70%, 90%, 95%, and 100% alcohol). Finally, the sections were cleared in xylene and mounted in D.P.X.
2. Golgi-Colonnier method (Blaesing et al., 2001)
   Small blocks 5 mm thick were also removed from both hemispheres of the brain for Golgi analysis. These blocks were taken from four regions namely Frontal, Temporal, Parietal, and Occipital. The left hemisphere was used for analysis by Golgi Colonnier procedure and the right hemisphere was used for analysis by the rapid Golgi method used by Valverde (1970). The left side cortical pieces from the above-mentioned regions were prechromed twice in 2.5% potassium dichromate for 60 min each treatment. The blocks were then kept in a 5% glutaraldehyde vol/vol and 2% potassium dichromate wt/vol solution at 4°C for 3 days for chroming before being transferred to 0.75% wt/vol solution of silver nitrate at 4°C for 2 days impregnation. Both chromation and impregnation steps were repeated further two times, with all the blocks washed in distilled water between solutions. After the completion of third and final impregnation, blocks were washed thoroughly in double distilled water. Blocks were then dehydrated in 50%, 70%, 90%, and 100% alcohol for 10–20 min in each solution followed by a 15 min immersion in 1:1 mixture of absolute alcohol and xylene. The blocks were then cleared in xylene

for 5–10 minutes and transferred to a mixture of xylene and molten paraffin wax (m.p. 56–58°C) at 56°C for 20 min. These were then transferred to pure molten paraffin wax (m.p. 56–58°C) at 56°C for a duration of 4 h (three changes of 1, 1, and 2 h each). Finally, the cortical blocks were embedded in paraffin wax. The blocks were sectioned at a thickness of 150–250 μm with the aid of rotatory microtome. The sections were deparaffinized in two changes of xylene (10 min each). They were then dehydrated in absolute alcohol for 20 min (two changes, 10 min each), cleared in xylene and mounted in D.P.X. mounting medium.

3. Rapid Golgi method (Valverde, 1970)
Cortical pieces from right hemisphere (5 mm in thickness) were immersed in an aqueous solution containing 2.33% wt/wt potassium dichromate and 0.19% wt/wt osmium tetroxide. A minimum of 20 mL of this solution was used for each piece. The tissue was kept in dark at room temperature for seven days. After chromation, the pieces were rinsed briefly in a small volume of 0.75% aqueous silver nitrate and stored for 24 h in a fresh volume of 0.75% silver nitrate. For each piece, 20 mL of the solution was used. The steps of chromation and silvering were repeated twice, with progressive lengthening of the silvering time and reduction of the chromation time. Between each step, blocks were blotted with tissue paper. The pieces were progressively dehydrated in different grades of alcohol for 15 min each and embedded in paraffin wax and sectioned by the same method as mentioned for Golgi-Colonnier method.

Spine density, spine length, diameter of spine head, and dendritic diameter were calculated from photomicrographs taken with the help of computer aided Nikon eclipse 80i microscope. The camera lucida drawings were made by simple light microscope equipped with camera lucida. All the drawings were scanned and corrected with the help of Adobe Photoshop computer software.

Statistical Approach

For calculation of spine density, numbers of spines were counted per 10 μm of dendritic segment. In this study, two types of spine density were calculated—Spine density 1 and Spine density 2. Spine density 1 (number of visible spines) was determined by counting all apparent spines along 10 μm of dendritic length. However some of the spines are obscured by opaque dendritic shaft; therefore in order to calculate "true" spine density, i.e. spine density 2, the formula given by Feldman and Peters (1979) was applied.

$$N = \frac{n\pi\left[(\mathrm{Dr}+\mathrm{Sl})^2-(\mathrm{Dr}+\mathrm{Sd})^2\right]}{\left[\frac{\theta}{90}.\pi(\mathrm{Dr}+\mathrm{Sl})^2\right]-2[(\mathrm{Dr}+\mathrm{Sl})\sin\theta(\mathrm{Dr}+\mathrm{Sd})]}$$

$n/D\mathrm{l}$ = spine density 1 and $N/D\mathrm{l}$ = spine density 2

where, N = true spine density; n = number of visible spines; Dr = radius of dendrite; Dl = dendritic length over which spines were counted; Sd = spine head diameter; Sl = length of spine, and θ = central angle.

Spine density 1 indicates only the number of visible spines and is under-representation of true figure since some of spines on the other side of circumference of dendrite are ignored (Horner and Arbuthnott, 1991) whereas spine density 2 is obviously more accurate estimate of true spine density. Therefore, spine density 2 values have been considered for comparing the data (spine density in pyramidal neurons of mongoose isocortex).

Statistical analysis (two-way ANOVA followed by Bonferroni *post hoc* comparison test) was done by the application of GraphPad Prism software 5.01 version.

RESULTS

The features of isocortex in *H. edwardsii* were broadly similar to eutherian cortex with a cell-free Layer I and clearly demarcated Layers II–VI (Fig. 1). On the basis of morphology, different types of neurons were observed in the isocortex in Golgi-impregnated sections. The identified types include: pyramidal, spinous bitufted and aspinous bitufted, spinous bipolar and aspinous bipolar, bipolar monotufted, spinous multipolar and aspinous multipolar, spinous unipolar and aspinous unipolar, and neurogliaform.

Pyramidal Cells

Pyramidal neurons constituted about two-thirds of total neocortical population. The percentage of different types of neurons observed in Frontal, Temporal, Parietal, and Occipital cortices are shown in Figure 2. The total percentage of pyramidal neurons was 71% in Frontal Cortex, 73% in Temporal, 76% in Parietal, and 82% in Occipital Cortex.

In this study, "classic" or "typical" pyramidal neurons reflected the six principal structural properties of "typical" pyramidal neurons in eutherians as listed by Nieuwenhuys (1994) though some pyramidal neurons in the four lobes of mongoose cortex were "atypical," i.e. deviated from "typical" one. The six principal structural properties characterizing "typical" pyramidal neurons in eutheria are presence of: dendritic spines, a radially oriented apical dendrite, a terminal bouquet of apical dendritic branches in Layer I, a skirt of basal dendrites, an axon descending to subcortical white matter, and intracortical axon collaterals. Some of the pyramidal neurons deviated from this "typical" morphology by showing one or more of following features: inverted somata, bifurcation of apical dendrites close to soma, poorly developed basal dendritic skirt, and lack of a terminal bouquet in Layer I and are designated as atypical pyramidal neurons. Atypical pyramidal cells constituted only 3–9% of all pyramidal neurons.

Layer wise and lobe wise observations of pyramidal neurons (Figs. 3 and 4) of mongoose isocortex with their spine density (spine density 1 and 2), spine length, and spine head diameter have been summed up in Tables (1–4). Spine density 2 of pyramidal neurons was found to be significantly different among regions [F (3, 12) = 15.84, $P < 0.0001$] and layers [F (4, 12) = 4.211, $P = 0.0038$] for apical dendrite, and region [F (3, 12) = 50.71, $P < 0.0001$] and layers [F (4, 12) = 4.669, $P = 0.0019$] for basal dendrites of pyramidal cells found in different layers inter alia the four

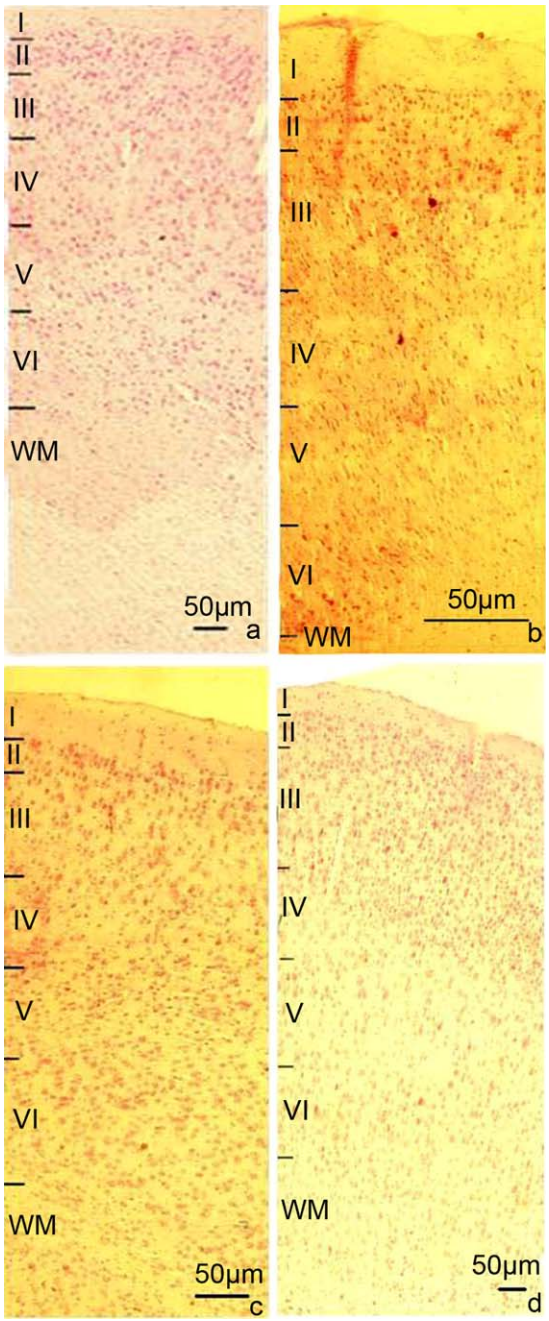

Fig. 1. Cresyl-violet stained section through (**a**) Frontal, (**b**) Temporal, (**c**) Parietal, and (**d**) Occipital region of mongoose isocortex. Cortical layers have been indicated; WM: White matter. [Color figure can be viewed in the online issue, which is available at wileyonlinelibrary.com.]

isocortical regions of mongoose by two-way ANOVA analysis (Table 5). The *post hoc* comparison result (Bonferroni) revealed the comparative account of differences in spine density among the four isocortical regions and layers of mongoose.

Apical Spine Density

The apical spine density 2 of pyramidal neurons of Layer II of Frontal and Parietal region showed significant differences (at $P < 0.001$) with Temporal region whereas spine density 2 in Layers III and VI of Frontal region ($P < 0.05$) and Parietal ($P < 0.01$) region were also significantly different with Temporal region. Apical spine density 2 of Layer IV of Parietal and Occipital region showed significant differences ($P < 0.001$) whereas differences in density of spines of Layer V of all the four isocortical regions of mongoose were insignificant ($P > 0.05$) (Fig. 5).

Basal Spine Density

Differences in basal spine density 2 of Temporal and Parietal region were significant for all the layers, i.e. Layers II, III, IV, V ($P < 0.001$) and VI ($P < 0.05$) whereas insignificant for Frontal vs. Parietal region ($P < 0.05$). Layers II, III, V ($P < 0.05$) and IV ($P < 0.001$) of Temporal and Layers II, III ($P < 0.05$), IV ($P < 0.01$) of Occipital region were significantly different in basal spine density 2 with Frontal region. Comparison of Parietal vs. Occipital was significant for Layers II, IV ($P < 0.001$), III ($P < 0.05$), and VI ($P < 0.01$). Differences among Occipital and Temporal for Layer III ($P < 0.01$) and V ($P < 0.001$) were also significant (Fig. 6).

Spine density showed an uneven distribution of spines not only within different regions of mongoose's brain but also among the layers of a region itself (Figs. 7 and 8). Highest spine densities per 10 μm (spine density 2) were observed in apical dendrites of Layer II pyramidal neurons and basal dendrites of Layer IV pyramidal neurons in temporal region of mongoose. The density of spine on pyramidal cells in Temporal region clearly outclassed the other regions (Figs. 5 and 6). The parietal region which showed longest and broadest spines on dendrites of pyramidal neurons was a complete laggard in terms of spine density as the pyramidal neurons of this region revealed the least density of spines.

DISCUSSION

The pyramidal neurons accounting for at least 70% of the total neocortical population in mammals form the principal element in neocortical circuit. The evolutionary trend of pyramidal neurons' development can be traced right from "extraverted" neurons observed in amphibian pallium; pyramid-like neurons in reptilian cortex (Luis de la Iglasia and Lopez Garcia, 1997; Srivastava et al., 2007, 2009b); in hippocampus of homing pigeon, chick (Tömböl et al., 2000); corticoid complex in strawberry finch (Srivastava et al., 2009a) to the well developed neocortical elements referred by Cajal as "psychic cells" (Nieuwenhuys, 1994). The different aspects of pyramidal cell microanatomy may influence different aspects of cellular, and systems function (Elston and DeFelipe, 2002; Häusser and Mel, 2003; Segev et al., 2001). The branching structure and spine density influence the total number of putative excitatory inputs sampled by cells. The present study focuses prime attention towards these morphological variables of pyramidal cells and deals with these features in following account.

In echidna, a monotreme, pyramidal neurons contributed to just one-third to one-half (34–49%) of the total number of neurons in cortex against 75–78% in rat cortex. Out of these pyramidal cells, many

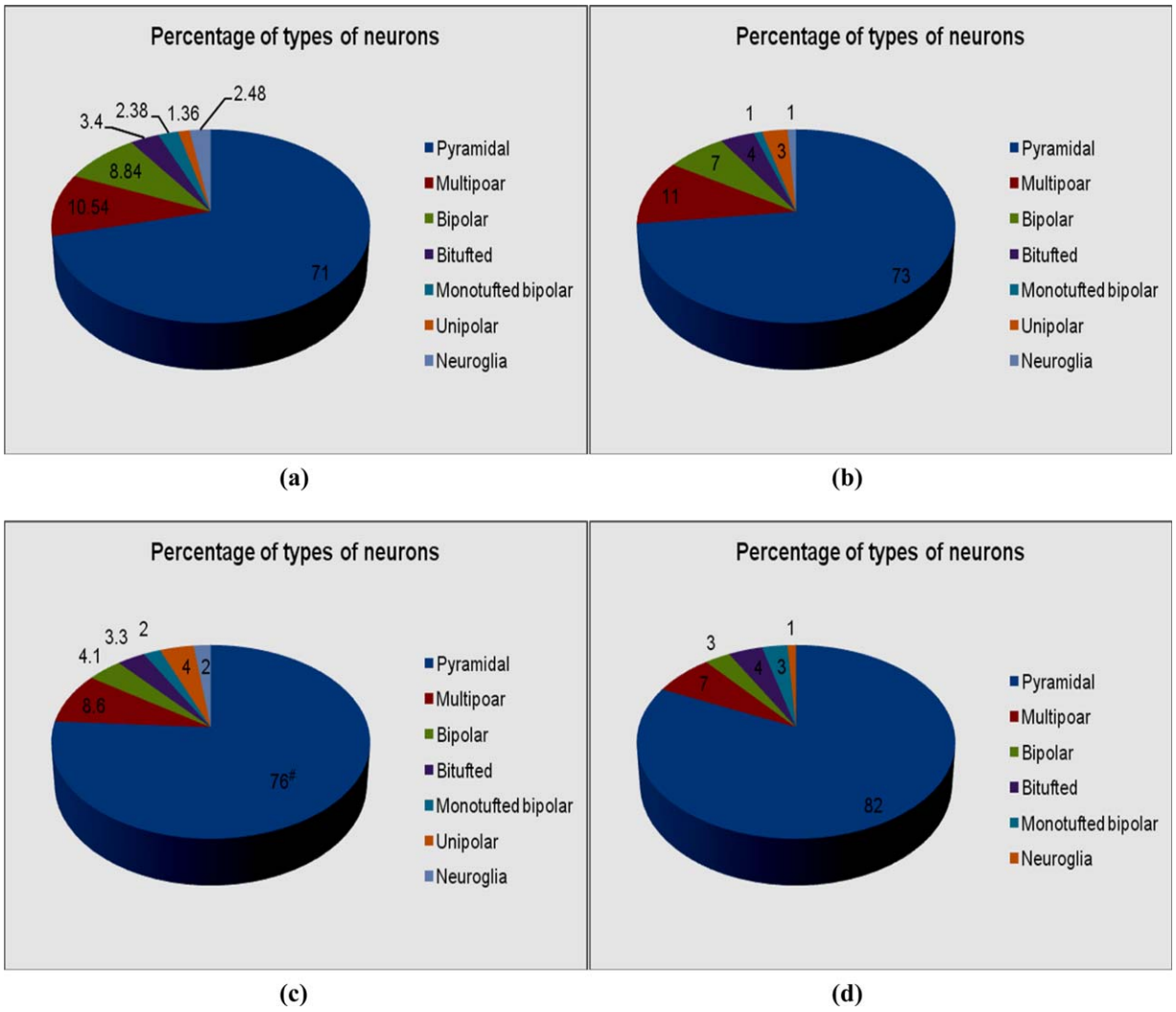

Fig. 2. Pie diagram showing percentage of different types of neurons observed in (**a**) Frontal, (**b**) Temporal, (**c**) Parietal, and (**d**) Occipital lobe of isocortex of *H. edwardsii*. (**#** Srivastava and Chauhan, 2010). [Color figure can be viewed in the online issue, which is available at wileyonlinelibrary.com.]

"atypical" pyramidal cells were seen, making up between 30 and 42% of all pyramidal neurons in echidna while only 7–9% in rat (Hassiotis and Ashwell, 2003). In marsupials, such as opossum (*Didelphis virginiania*), the predominant cell type in cortex is pyramidal neuron and their morphology is similar to "classical" or "typical" pyramidal cells seen in eutheria (Walsh and Ebner, 1970). Within eutherians, pyramidal neurons escalate further in frequency and continue to dominate the population of neurons in rodents (Connor et al., 1982; Ferrer et al., 1986; Petit et al., 1988), lagomorphs (Ferrer et al., 1986; Mathers, 1979), carnivores (Ferrer et al., 1986; Zervas and Walkely, 1999), and primates (Elston, 2003; Elston et al., 1999; Hof et al., 2000; Sherwood et al., 2003). In *H. edwardsii* the percentage of pyramidal cells was observed to be in the range of 73–82% among all regions which is higher than in rat followed by echidna (Hassiotis and Ashwell, 2003).

The thickness of apical and basal dendrites of pyramidal neurons was found to vary within and among the four regions studied in mongoose. Apical dendritic thickness varied from 0.6 to 5.2μm with occipital lobe showing the thinnest one (up to 2.7 μm). In most of the cases, dendritic diameter increased from outer to inner layers with some exceptions. In case of basal dendrite, it was observed that the thickness varied from 0.40 to 3.6 μm. These findings when compared to those reported in motor and somatosensory cortex of monotreme and rodent (Hassiotis and Ashwell, 2003) and parietal cortex of chiropteran (Srivastava and Pathak, 2010) show a remarkable difference in both apical and basal dendrites and show an increasing order from echidna to bat, rat, and mongoose in case of apical dendrites. But, in case of basal dendrite, bat showed higher thickness than rat. Thus, it can be perceived that the thickness of apical and basal dendrites increases from primitive monotremes to advanced eutherians but basal dendrites apparently do not follow the suit.

Dendritic spines provide modifiable sites of excitable synaptic input and account for 70–95% of the synaptic

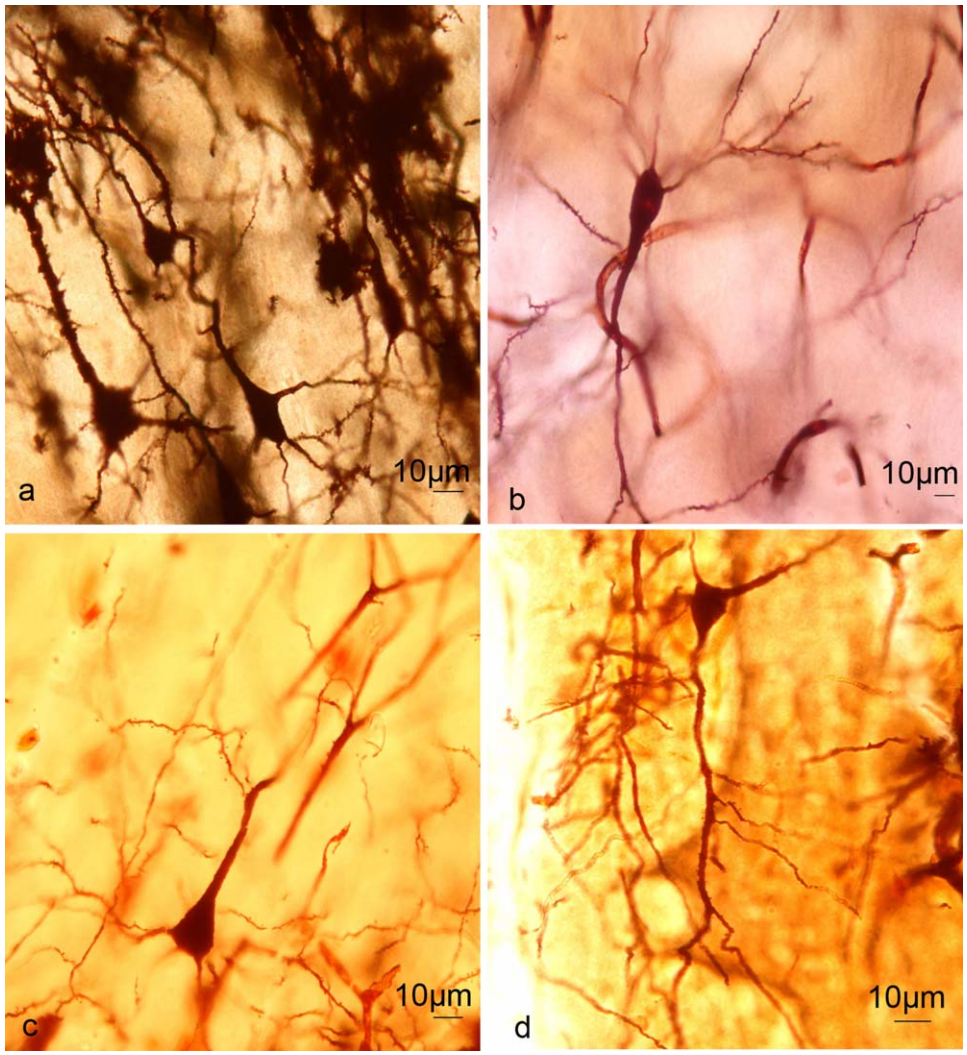

Fig. 3. Photomicrograph showing pyramidal neurons observed in (**a**) Frontal, (**b**) Temporal, (**c**) Parietal, and (**d**) Occipital region of mongoose isocortex. [Color figure can be viewed in the online issue, which is available at wileyonlinelibrary.com.]

input to eutherian pyramidal neurons (Horner, 1993; Nieuwenhuys, 1994). In mature animals, activity-dependent changes of the postsynaptic structure are thought to contribute to the plasticity of neural circuits and possibly to learning and memory (Yuste and Bonhoeffer, 2001). Spine density may be directly linked to physiological processes like hormonal changes, hibernation, and behavioral processes like learning (Segal and Andersen, 2000). The length and morphology of dendritic spines on echidna pyramidal neurons was purported to be very similar to that seen in therian mammals (length along spines ranging from 1.5 to 3.5μm; morphology ranging from spikes to elongated clubs to mushrooms), but spine density was significantly lower on both apical and basal dendrites of Layer V pyramidal neurons in motor cortex (Hassiotis and Ashwell, 2003). Spines in mongoose appeared to be morphologically similar to those reported in other mammals with shapes varying from spike-like to club-shaped and mushroom-shaped with elongated neck. The lengths of spines were markedly variable ranging from 0.5 to 3.7 μm with longest spines revealed in Layer IV of parietal isocortex in mongoose. The diameters of spine heads were also of differential nature with parietal region again showing the largest spine heads (0.6–1.8 μm) as compared to the other three regions (0.18–1.5 μm).

Elston et al. (1999) opined that the greater number of spines on the basal dendrites of pyramidal neurons in "higher" areas, and their more widespread dendritic trees may allow an increased degree of association, allowing integration of different features over larger regions of cortex in marmoset monkey. Spine density 2 of pyramidal neurons was found to be significantly different among both apical and basal dendrites of pyramidal cells found in different layers inter alia the four isocortical regions of mongoose brain and moreover the differences were more prominent in basal spine density in comparison to apical spine density indicating that basal dendrites bear more spines and hence facilitate more synaptic connectivity.

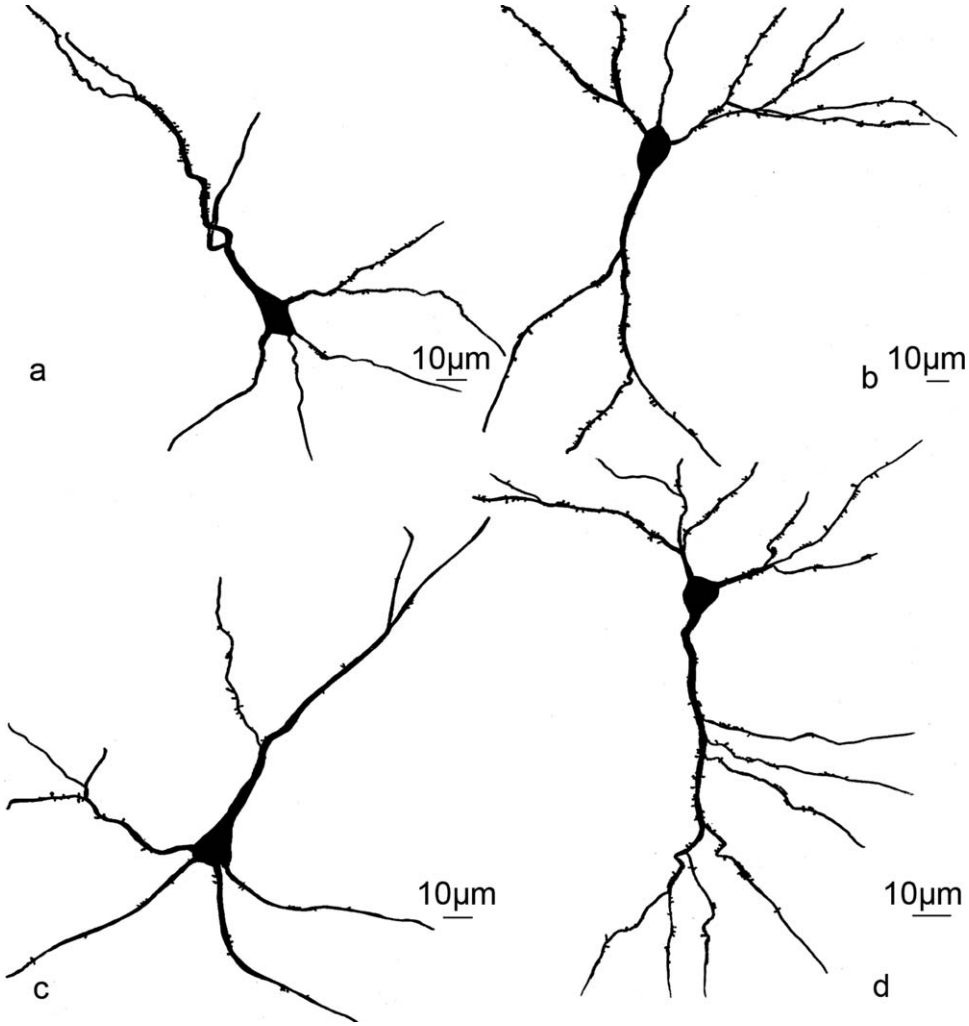

Fig. 4. Camera lucida drawings of pyramidal neurons observed in (**a**) Frontal, (**b**) Temporal, (**c**) Parietal, and (**d**) Occipital region of mongoose isocortex.

TABLE 1. Characteristic features of pyramidal neurons identified in Frontal lobe of mongoose, Herpestes edwardsii

Layer	Spine density 1 (number of visible spines per 10 μm of dendritic length, *n/D*l)	Spine density 2 (true estimate of spine density per 10 μm of dendritic length, *N/D*l)	Dendritic diameter (μm)	Spine length (μm)	Diameter of spine head (μm)
II A	4.2 ± 1.30	16.01 ± 5.42	1.08–1.44	0.6–0.9	0.35–0.53
II B	5.8 ± 3.03	13.38 ± 4.99	0.56–1.74	0.5–1.06	0.18–0.35
III A	3.4 ± 1.14	8.47 ± 3.71	0.9–2.44	0.6–2.38	0.53–0.88
III B	2.6 ± 1.34	7.51 ± 2.55	0.6–1.4	0.6–1.23	0.53–0.70
IV A	7.2 ± 3.27	16.21 ± 5.16	1.5–3.9	1.4–2.64	0.26–0.35
IV B	7.4 ± 1.34	14.84 ± 2.02	0.68–1.4	0.6–1.76	0.18–0.35
V A	6.2 ± 3.27	13.79 ± 7.27	0.94–1.7	0.88–1.58	0.35–0.70
V B	7.6 ± 2.07	12.80 ± 4.74	0.4–0.96	0.97–2.55	0.4–1.50
VI A	6.8 ± 1.92	14.45 ± 5.04	0.86–2.06	0.97–1.67	0.18–0.48
VI B	8.2 ± 2.94	13.91 ± 3.94	0.48–1.0	1.0–1.94	0.26–0.44

Spine density represented as mean ± SD, A, apical dendrite; B, basal dendrite; Dl, dendritic length over which spines were counted; *n*, number of visible spines; *N*, estimate of "true" total spines derived by formula by Feldman and Peters (1979).

The distribution of spines over the dendritic field is not uniform but uneven in hippocampus of rat (Horner and Arbuthnott, 1991). This is well in tune with the present data on spine density which also revealed uneven distribution of spines not only within different regions of mongoose's brain but also among the layers of a region itself. Highest spine densities per 10 μm (spine density 2) were observed in apical dendrites of Layer II pyramidal neurons and basal dendrites of Layer IV pyramidal neurons, in temporal region of

TABLE 2. Characteristic features of pyramidal neurons identified in Temporal lobe of mongoose, Herpestes edwardsii

Layers	Spine density 1 (number of visible spines per 10 μm of dendritic length, *n*/*D*l)	Spine density 2 (true estimate of spine density per 10 μm of dendritic length, *N*/*D*l)	Dendritic diameter (μm)	Spine length (μm)	Diameter of spine head (μm)
II A	6.2 ± 1.64	34.26 ± 7.64	1.08–2.76	0.7–1.23	0.62–0.97
II B	8 ± 1.87	23.51 ± 8.15	0.92–1.68	1.1–1.32	0.6–0.79
III A	8 ± 2.91	22.47 ± 9.41	1.4–1.86	1.3–1.94	0.62–1.1
III B	8.6 ± 1.51	30.9 ± 7.38	1.21–1.90	1.32–2.11	0.88–1.5
IV A	3.2 ± 0.83	17.3 ± 10.94	1.36–4.9	0.79–1.76	0.7–1.1
IV B	4.8 ± 1.09	31.98 ± 11.92	1.36–1.84	0.79–1.23	0.70–1.14
V A	5.4 ± 2.50	19.75 ± 5.57	1.06–2.4	0.53–1.76	0.44–0.88
V B	7.6 ± 2.30	24.04 ± 9.7	1.6–2.06	1.1–1.76	0.7–1.23
VI A	5.2 ± 2.28	28.44 ± 13.63	1.16–5.22	0.97–1.32	0.7–0.88
VI B	5 ± 1.58	17.01 ± 5.99	1.08–1.75	1.3–1.76	0.8–1.23

Spine density represented as mean ± SD; A, apical dendrite; B, basal dendrite; Dl, dendritic length over which spines were counted; *n*, number of visible spines; *N*, estimate of "true" total spines derived by formula by Feldman and Peters (1979).

TABLE 3. Characteristic features of pyramidal neurons identified in Parietal lobe of mongoose, Herpestes edwardsii

Layers	Spine density 1 (number of visible spines per 10 μm of dendritic length, *n*/*D*l)	Spine density 2 (true estimate of spine density per 10 μm of dendritic length, *N*/*D*l)	Dendritic diameter (μm)	Spine length (μm)	Diameter of spine head (μm)
II A	2.8 ± 0.83	13.72 ± 3.2	1.7–2.94	1.4–2.5	0.9–1.5
II B	2 ± 0.70	5.66 ± 0.88	1.0–2.4	1.4–1.8	0.7–1.0
III A	3.2 ± 0.83	7.33 ± 1.2	1.7–4.5	1.6–2.7	1.2–1.7
III B	2.4 ± 1.51	7.15 ± 3.69	1.5–3.2	0.8–1.56	0.6–1.07
IV A	3.6 ± 1.14	8.90 ± 3.23	2.2–4.7	2.0–3.7	1–2
IV B	2.6 ± 1.14	5.3 ± 1.72	1.1–2.9	1.0–1.78	1.1–1.8
V A	6.8 ± 0.83	13.69 ± 2.26	1.82–4.94	1.0–2.9	1.1–1.4
V B	2.6 ± 1.14	5.38 ± 2.1	0.9–2.7	1.2–1.7	0.9–1.4
VI A	7.4 ± 2.19	13.08 ± 5.3	0.75–3.76	1.4–2.6	0.9–1.6
VI B	2.2 ± 1.30	6.02 ± 1.06	0.98–2.1	0.78–1.56	0.6–0.92

Spine density represented as mean ± SD; A, apical dendrite; B, basal dendrite; Dl, dendritic length over which spines were counted; *n*, number of visible spines; *N*, estimate of "true" total spines derived by formula by Feldman and Peters (1979).

TABLE 4. Characteristic features of pyramidal neurons identified in Occipital lobe of mongoose, Herpestes edwardsii

Layers	Spine density 1 (number of visible spines per 10 μm of dendritic length, *n*/*D*l)	Spine density 2 (True estimate of spine density per 10 μm of dendritic length, *N*/*D*l)	Dendritic diameter (μm)	Spine length (μm)	Diameter of spine head (μm)
II A	7.6 ± 2.70	22.2 ± 8.79	0.9–1.1	0.8–1.14	0.35–0.53
II B	11.4 ± 2.30	24.84 ± 6.22	0.36–0.48	0.53–1.06	0.18–0.35
III A	5.2 ± 1.30	13.68 ± 4.14	0.96–1.34	0.79–2.02	0.53–0.88
III B	10 ± 2.34	18.75 ± 4.18	0.66–1.2	1.5–2.46	0.5–0.7
IV A	13.4 ± 6.58	27.94 ± 13.67	0.56–0.8	0.79–1.06	0.26–0.35
IV B	17.6 ± 6.80	28.48 ± 11.55	0.34–0.56	0.88–1.58	0.18–0.35
V A	4.2 ± 2.28	11.76 ± 5.76	1.52–2.66	0.88–1.41	0.35–0.70
V B	2.8 ± 1.30	7.50 ± 4.39	0.83–2.24	1.32–1.94	0.53–1.5
VI A	10.2 ± 3.11	18.39 ± 5.85	0.44–0.84	0.97–1.23	0.18–0.35
VI B	12 ± 3.80	20.06 ± 4.32	0.3–0.64	0.88–1.32	0.26–0.44

Spine density represented as mean ± SD; A, apical dendrite; B, basal dendrite; Dl, dendritic length over which spines were counted; *n*, number of visible spines; *N*, estimate of "true" total spines derived by formula by Feldman and Peters (1979).

TABLE 5. Two-way ANOVA analysis of density of dendritic spines on pyramidal neurons of Frontal, Temporal, Parietal and Occipital region of mongoose isocortex

	Spine density 2 (per 10 μm of dendritic length)				Two-way ANOVA analysis		
Layer	Frontal	Temporal	Parietal	Occipital	*F* value	d.f.	*P* value
II A	16.01 ± 5.42	34.26 ± 7.64[a]	13.72 ± 3.2	22.2 ± 8.79	Interaction = 2.020		Significant ($P = 0.0328$)
III A	8.47 ± 3.71	22.47 ± 9.41[a]	7.33 ± 1.2	13.68 ± 4.14	Region = 15.84	$n_1 = 3$, $n_2 = 12$	Significant ($P < 0.0001$)
IV A	16.21 ± 5.16	17.3 ± 10.94	8.90 ± 3.23	27.94 ± 13.67[a]			
V A	13.79 ± 7.27	19.75 ± 5.57	13.69 ± 2.26	11.76 ± 5.76	Layers=4.211	$n_1 = 4$, $n_2 = 12$	Significant ($P = 0.0038$)
VI A	14.45 ± 5.04	28.44 ± 13.63[a]	13.08 ± 5.3	18.39 ± 5.85			
II B	13.38 ± 4.99	23.51 ± 8.15	5.66 ± 0.88	24.84 ± 6.22[a]	Interaction = 3.503		Significant ($P = 0.0003$)
III B	7.51 ± 2.55	30.9 ± 7.38[a]	7.15 ± 3.69	18.75 ± 4.18	Region = 50.71	$n_1 = 3$, $n_2 = 12$	Significant ($P < 0.0001$)
IV B	14.84 ± 2.02	31.98 ± 11.92[a]	5.3 ± 1.72	28.48 ± 11.55			
V B	12.80 ± 4.74	24.04 ± 9.7[a]	5.38 ± 2.1	7.50 ± 4.39	Layers=4.669	$n_1 = 4$, $n_2 = 12$	Significant ($P = 0.0019$)
VI B	13.91 ± 3.94	17.01 ± 5.99	6.02 ± 1.06	20.06 ± 4.32[a]			

Values represented as means ± SD; A, apical dendrite; B, basal dendrite; d.f., degree of freedom.
[a]Indicating significant differences

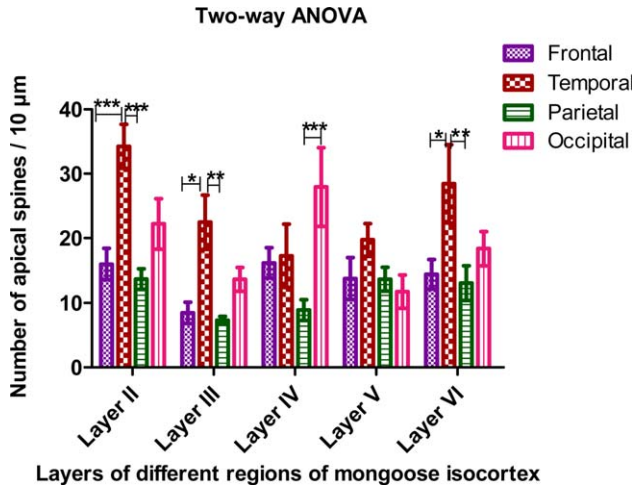

Fig. 5. Density of spines (spine density 2) on apical dendrite of pyramidal neurons in the isocortex of mongoose. Values represented as mean ± SEM. SEM: Standard error of mean, Number of * shows the degree of significance between the indicated regions within different layers. [Color figure can be viewed in the online issue, which is available at wileyonlinelibrary.com.]

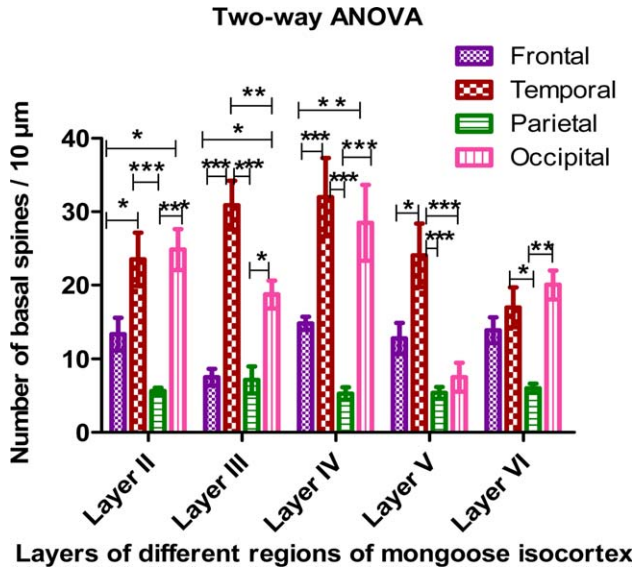

Fig. 6. Density of spines (spine density 2) on basal dendrite of pyramidal neurons in the isocortex of mongoose. Values represented as mean ± SEM. SEM: Standard error of mean, Number of * shows the degree of significance between the indicated regions within different layers. [Color figure can be viewed in the online issue, which is available at wileyonlinelibrary.com.]

mongoose. The density of spine on pyramidal cells in temporal region clearly outclassed the other regions and these differences were observed to be significant for both apical and basal spine density. It was interesting to note that the parietal region which showed longest and broadest spines on dendrites of pyramidal neurons was a complete laggard in terms of spine density as the pyramidal neurons of this region revealed the least density of spines. It could be possible that the long and broad spines of parietal region were so as to compensate for the scarcity of spines. Also, the

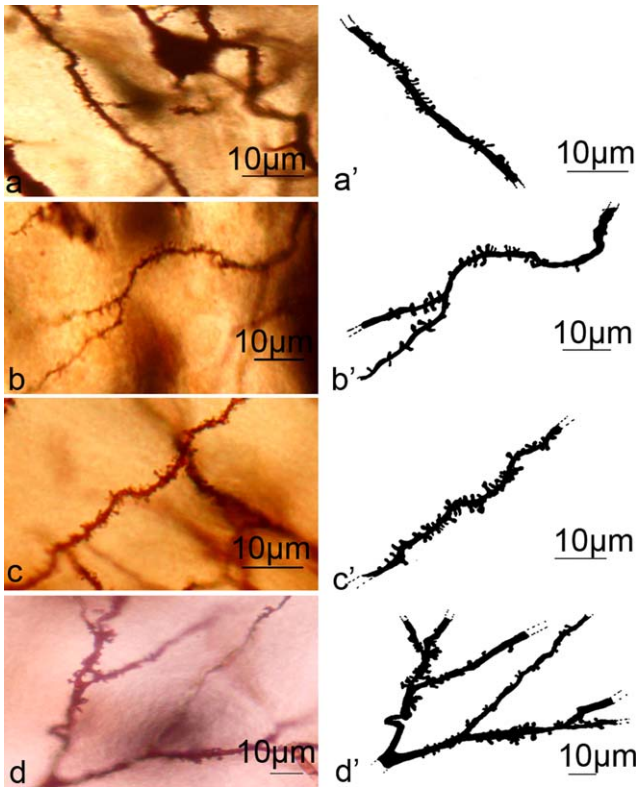

Fig. 7. Photomicrographs and drawings illustrating spinous processes sampled in selected apical (**a**, **a**′), basal dendrite (**b**, **b**′) of layer IV typical pyramidal neuron of Frontal region and apical (**c**, **c**′), basal dendrite (**d**, **d**′) of layer II typical pyramidal neuron of Temporal region in mongoose. [Color figure can be viewed in the online issue, which is available at wileyonlinelibrary.com.]

significant differences in laminar distribution of spines, which act as site for long-term, stable memory in neurons (Holtmaat et al., 2005) indicate that all pyramidal cells present in different layers are not equally functional and differences do exist in activity among different layers of a region itself. From the differences in spine densities in different layers of isocortex of mongoose, it can be inferred that different layers of same region contribute differentially in their functions. As far as regions are concerned it seems likely that Temporal region possessing highest spine density contributes more towards the functioning of isocortex in mongoose and might play significant role in predatory nature of mongoose since temporal region in mammals is known to be involved in processing sensory inputs such as auditory perception, object perception, and recognition (Beauchamp et al., 2002; Buffalo et al., 2006) and even involved in regulating social behavior and signaling in monkeys (Myers, 1972) which might help mongoose to recognize and perceive its prey within the environment. Relative abundance of "typical" pyramidal neurons increases from primitive to advanced mammals and of "atypical" cells, decreases from primitive to advanced ones (Nieuwenhuys, 1994). In mongoose, percentage of "atypical" pyramidal cells is only 3–9% showing advanced nature of the isocortex as compared to 25.38% in Parietal cortex of Indian bat (Srivastava and Pathak, 2010) and 30%

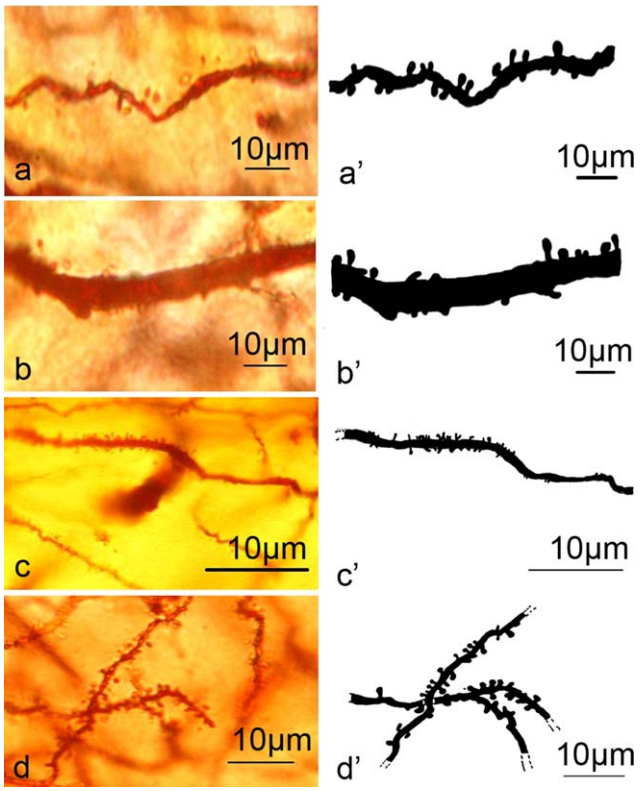

Fig. 8. Photomicrographs and drawings illustrating spinous processes sampled in apical (**a**, **a**′), basal (**b**, **b**′) of layer V typical pyramidal neuron of Parietal region and apical (**c**, **c**′), basal dendrite (**d**, **d**′) of layer IV typical pyramidal neuron of Occipital region in mongoose. [Color figure can be viewed in the online issue, which is available at wileyonlinelibrary.com.]

in Frontal cortex of echidna (Hassiotis and Ashwell, 2003).

Medial Temporal lobe in mammals consists of structures vital for declarative memory comprising of semantic memory (facts) and episodic memory (events) (Smith and Kosslyn, 2007) whereas Occipital region is the visual processing center (Caveni and Saeti, 2001). Jacobs and Scheibel (2002) proposed that regional specialization in pyramidal cell structure may offer advantages for specialized functioning. Therefore highly spinous pyramidal cells of Temporal and Occipital region in mongoose indicate higher functioning of these two lobes which might help in better visual processing as well as retention of declarative memories. The relative abundance of pyramidal neurons with increased diameter of dendrites and high spine density on dendrites of pyramidal neurons seem to be well in accordance with the predatory mode of life of mongoose allowing increased degree of association, integration of different features over all the regions of isocortex. These features perhaps help mongoose keep pace with its environment for getting its prey and defending itself against predators.

CONCLUSION

The spine density which can be considered to be a measure of complexity of a given neuronal network has been found to differ among the cortical layers and regions of mongoose isocortex. This variation in spine density observed in present study is believed to contribute to functional differences among the four regions and layers. Apical spine density of Layer II and basal spine density of Layer IV within Temporal region were found to be highest and showed significant differences which points toward the efficacy of Temporal region and its contribution toward functionality of mongoose isocortex. The present finding provides a valuable and comparative set of information describing the differences in distribution of spines on both apical and basal dendrites of pyramidal neurons within all the four regions and different layers of mongoose isocortex.

ACKNOWLEDGMENTS

The authors thank the Head of Department of Zoology, University of Allahabad, Allahabad for providing essential facilities for the present investigation.

REFERENCES

Beauchamp MS, Lee KE, Haxby JV, Martin A. 2002. Parallel visual motion processing streams for manipulable objects and human movements. Neuron 34:149–159.

Benavides-Piccione R, Hamzei-Sichani F, Ballesteros-Yáñez I, DeFelipe J, Yuste R. 2006. Dendritic size of pyramidal neurons differ among mouse cortical regions. Cereb Cortex 16:990–1001.

Blaesing B, Nossoll M, Teuchert Noodt G, Dawirs RR. 2001. Postnatal maturation of prefrontal pyramidal neurons is sensitive to a single early dose of methamphetamine in gerbil (*Meriones unguiculatus*). J Neural Transm 103:101–103.

Buffalo EA, Bellgowan PSF, Martin A. 2006. Distinct roles for medial temporal lobe structures in memory for objects and their locations. Learn Mem 13:638–643.

Caveni MP, Saeti SW. 2001. Visuoperceptive impairment in adults with occipital lobe epilepsy. Epilepsy Behav 205–206.

Chagnac-Amitai Y, Luhmann HJ, Prince DA. 1990. Burst generating and regular spiking layer V Pyramidal neurons of rat neocortex have different morphological features. J Comp Neurol 296:598–613.

Connor JR, Beban SE, Hopper PA, Hansen B, Diamond MC. 1982. A Golgi study of the superficial pyramidal cells in the somatosensory cortex of socially reared old adult rats. Exp Neurol 76:35–45.

Elston GN. 2003. The pyramidal neuron in occipital, temporal and prefrontal cortex of the owl monkey (*Aotus trivirgatus*): Regional specialization in cell structure. Eur J Neurosci 17:1313–1318.

Elston GN, DeFelipe J. 2002. Spine distribution in cortical pyramidal cells: A common organizational principle across species. Prog Brain Res 136:109–133.

Elston GN, Tweedale R, Rosa MGP. 1999. Cellular heterogeneity in cerebral cortex. A study of the morphology of pyramidal neurones in visual areas of marmoset monkey. J Comp Neurol 415:33–51.

Elston GN, Elston A, Casagrande V, Kaas JH. 2005. Areal specialization of pyramidal cell structure in the visual cortex of the tree shrew: A new twist revealed in the evolution of cortical circuitry. Exp Brain Res 163:13–20.

Feldman ML. 1984. Morphology of the neocortical pyramidal neuron. In: Peters A, Jones EG, editors. Cerebral cortex, Vol. I: Cellular components of the cerebral cortex. New York: Plenum Press. pp. 123–200.

Feldman ML, Peters A. 1979. A technique for estimating total spine numbers on Golgi-impregnated dendrites. J comp Neurol 188:527–542.

Ferrer I, Fabregues I, Condom E. 1986. A Golgi study of the sixth layer of the cerebral cortex. II. The gyrencephalic brain of Carnivora, Artiodactyla and Primates. J Anat 146:87–104.

Ferrer I, Fabregues I, Condom E. 1987. A Golgi study of the sixth layer of the cerebral cortex. III. Neuronal changes during normal and abnormal cortical folding. J Anat 152:71–82.

Fitzpatrick DC, Henson OW. 1994. Cell types in mustached bat auditory cortex. Brain Behav Evol 43:79–91.

Garey LJ, Saini KD. 1981. Golgi studies of the neuronal development of neurons in the lateral geniculate nucleus of the monkey. Exp Brain Res 44:117–128.

Garey LJ, Winkelmann E, Brauer K. 1985. Golgi and Nissl studies of the visual cortex of the Bottlenose Dolphin. J Comp Neurol 240:305–321.
Gilbert CD, Kelly JP. 1975. The projections of cells in different layers of the cat's visual cortex. J Comp Neurol 163:81–106.
Hassiotis M, Ashwell KW. 2003. Neuronal classes in the isocortex of a monotreme, the Australian echidna (*Tachyglossus aculeatus*). Brain Behav Evol 61:6–27.
Häusser M, Mel B. 2003. Dendrites: Bug or feature? Curr Opin Neurobiol 13:372–383.
Hof PR, Glezer II, Condé F, Flagg R, Rubin MB, Nimchinsky EA, Vogt Weisenhorn DM. 1999. Cellular distribution of calcium-binding proteins paravalbumin, calbindin, and calretinin in the neocortex of mammals: Phylogenetic and developmental patterns. J Chem Neuroanat 16:77–116.
Hof PR, Glezer II, Nimchinsky EA, Erwin JM. 2000. Neurochemical and cellular specializations in mammalian neocortex reflect phylogenetic relationships: Evidence from primates, cetaceans and artiodactyls. Brain Behav Evol 55:300–310.
Holtmaat AJGD, Trachtenberg JT, Wilbrech, L, Shepherd GM, Zhang X, Knott GW, Svoboda K. 2005. Transient and persistent dendritic spines in the neocortex in vivo. Neuron 45:279–291.
Horner C. 1993. Plasticity of the dendritic spine. Prog Neurobiol 41:281–321.
Horner CH, Arbuthnott E. 1991. Methods of estimation of spine density—Are spines evenly distributed throughout the dendritic field? J Anat 177:179–184.
Jacobs B, Scheibel AB. 2002. Regional dendritic variation in primate cortical pyramidal cells. In: Schüz A, Miller R, editors. Cortical areas: Unity and diversity. London: Taylor & Francis. Pp. 111–131.
Luis de la Iglasia JA, Lopez Garcia C. 1997. A Golgi study of the principal projection neurons of the medial cortex of the lizard *Podarcis hispanica*. J Comp Neurol 385:528–564..
Lund JS, Henry GH, MacQueen CL, Harvey AR. 1979. Anatomical organization of the primary visual cortex (area 17) of the cat: A comparison with area 17 of macaque monkey. J Comp Neurol 184:599–618.
Mathers LH, Jr. 1979. Postnatal development in the rabbit visual cortex. Brain Res 168:21–29.
Mitra NL. 1955. Quantative analysis of cell types in mammalian neocortex. J Anat 89:467–483.
Myers RE. 1972. Role of prefrontal and anterior temporal cortex in social behavior and affect in monkeys. Acta Neurobiol Exp 32:567–579.
Nieuwenhuys R. 1994. The Neocortex. An overview of its evolutionary development, structural organization and synaptology. Anat Embryol 190:307–337.
Petit TL, Le Boutilier JC, Gregorio A, Libstug H. 1988. The pattern of dendritic development in the cerebral cortex of the rat. Brain Res Dev Brain Res 41:209–219.
Radtke-Schuller S. 2001. Neuroarchitecture of the auditory cortex in the rufous horseshoe bat (*Rhinolophus rouxi*). Anat Embryol 204:81–100.
Segal M, Andersen P. 2000. Dendritic spines shaped by synaptic activity. Curr Opin Neurobiol 10:582–586.
Segev I, Burke RE, Hines M. 2001. Compartmental models of complexneurons. In: Koch C, Segev I, editors. Methods in neuronal modeling. London: MIT Press. pp. 93–136.
Sherwood CC, Lee PWH, Rivara CB, Holloway RL, Gilissen EPE, Simmons RMT, Hakeem A, Allman JM, Erwin JM, Hof PR. 2003. Evolution of specialized pyramidal neurons in primate visual and motor cortex. Brain Behav Evol 61:28–44.
Smith EE, Kossyln SM. 2007. Cognitive psychology: Mind and brain, Vo. 21. New Jersey: Prentice Hall. pp.194–199.
Srivastava UC, Chauhan P. 2010. Morphological differences among pyramidal neurons in parietal lobe of a carnivore, Indian mongoose, *Herpestes edwardsii*. Natl Acad Sci Lett 33:89–94.
Srivastava UC, Pathak SV. 2010. Interlaminar differences in the pyramidal cell phenotype in parietal cortex of an indian bat, *Cynopterus sphinx*. Cell Mol Biol 56:OL1410–OL1426.
Srivastava UC, Srivastava M. 2011. Interlaminar variations among pyramidal neurons in isocortex of a rodent, Indian squirrel, *Funambulus pennanti* Robert Charles Wroughton, 1905. Proc Natl Acad Sci India Sect B 81:260–279.
Srivastava UC, Maurya RC, Shishodiya U. 2007. Cytoarchitecture and morphology of the different neuronal types of the cerebral cortex of an Indian lizard (*Mabouia carinata*). Proc Natl Acad Sci India 77:331–347.
Srivastava UC, Chand P, Maurya RC. 2009a. Neuronal classes in the corticoid complex of the telencephalon of the strawberry finch, *Estrilda amandava*. Cell Tissue Res 336:393–409.
Srivastava UC, Maurya RC, Chand P. 2009b. Cyto-architecture and neuronal types of the dorsomedial cerebral cortex of the common Indian wall lizard (*Hemidactylus flaviviridis*). Arch Ital Biol 147:21–35.
Tömböl T, Davies DC, Németh A, Sebestény T, Alpár A. 2000. A comparative Golgi study of chicken (*Gallus domesticus*) and homing pigeon (*Columba livia*) hippocampus. Anat Embryol 201:85–101.
Tunturi AR. 1971. Classification of neurons in the ectosylvian auditory cortex of the dog. J Comp Neurol 142:153–166.
Valverde F. 1970. The Golgi method, a tool for comparative structural analysis. In: Nauta WJH, Ebbesson SO, editors. Contemporary research methods in neuroanatomy. New York: Springer-Verlag. pp. 12–31.
Von Economo C. 1927. Zellaufbau der grossnhirnrinde des Menschen. Verlag Von Julius. Berlin: Springer.
Walsh TM, Ebner FF. 1970. The cytoarchitecture of somatic sensorymotor cortex in the opossum (*Didelphis marsupialis virginiana*): A Golgi study. J Anat 107:1–18.
Yuste R, Bonhoeffer T. 2001. Morphological changes in dendritic spines associated with long-term synaptic plasticity. Annu Rev Neurosci 24:1071–1089.
Zervas M, Walkley SU. 1999. Ferret pyramidal cell dendritogenesis: Changes in morphology and ganglioside expression during cortical development. J Comp Neurol 413:429–448.